

SEE characteristics of small feature size devices by using laser backside testing*

Feng Guoqiang(封国强)[†], Shangguan Shipeng(上官士鹏), Ma Yingqi(马英起),
and Han Jianwei(韩建伟)

Center for Space Science and Applied Research, Chinese Academy of Sciences, Beijing 100190, China

Abstract: This paper presents single event upset (SEU) and single event latch-up (SEL) characteristics of small feature size devices by laser backside testing method, which is dedicated to dealing with the increasing metal layers on the front side of integrated circuits. The influence of test data pattern on SEU threshold and cross-section is investigated. The supply current state of micro latch-up for deep sub-micron SRAM is described. The laser energy thresholds were correlated to heavy ion thresholds LET to determine an empirical relationship between laser energy threshold and heavy ion LET. This empirical relationship was used to estimate the equivalent laser LETs for devices fabricated in small feature sizes. Moreover, the SEU of a Power PC CPU fabricated with 90 nm SOI CMOS process has been tested, which indicates that the laser backside method could be used to evaluate SOI small feature size devices.

Key words: SEU; SEL; laser; backside

DOI: 10.1088/1674-4926/33/1/014008

EEACC: 2570

1. Introduction

As SEE simulation with a pulsed laser is a simple and convenient method that does not damage the test devices, and has many advantages absent in accelerators, for example, capable of detecting sensitive cells with high resolution and diagnosing temporal characteristics of an upset transmitting in logic circuits, it has found broad applications in SEE studies and exhibits particular merits in measuring SEE sensitivity, selecting radiation hardened devices in batches and validating radiation protection measurements^[1-5]. Theoretical works about simulation by laser are mainly investigations of the mechanism and methods of pulsed laser energy deposition in semiconductor devices^[6,7], nonlinear effects of interaction, characteristics of laser ionization tracks^[8], as well as computer simulation of laser induced SEU^[9,10]. Compared to a traditional laser front-side approach, as an increasing number of metal layers, another way is the laser backside technique to test SEE of high density devices^[11,12].

In particular, as the device feature sizes scale down, the SEE phenomena is becoming complex, for instance, the lower threshold LET, the larger cross-section, multiple-bit upset (MBU), extreme latch-up susceptibility and micro latch-up, etc^[13-18]. In this paper, SEE characteristics of several small feature sizes devices have been examined by laser backside testing. Pulsed lasers have different ionization tracks from those of heavy ions, which will affect the charge collection in sensitive region and eventually affect the SEE sensitivity measurements. However, a large number of experimental examinations have shown that both heavy ions and pulsed lasers can induce similar transient effects in semiconductor devices^[19,20]. Moreover, the SEE sensitivity of devices is generally characterized by LET threshold and SEE cross-sections as a function

of LET. Therefore, in the following the laser energy thresholds were correlated to heavy ion thresholds LET to determine an empirical relationship between laser energy threshold and heavy ion LET. This empirical relationship was used to estimate the equivalent laser LET for devices built in small feature sizes.

2. Experimental

In this study, two commercial SRAMs and one industrial CPU from Hitachi (sample #1), IDT (sample #2) and Freescale (sample #3) were conducted. The function and main technical parameters of all the tested components are listed in Table 1. Two SRAMs are available in a wire-bond plastic package. The backside of the SRAM plastic and metallic lead frames had been partially removed to exposure the silicon substrate surface, as shown in Fig. 1. The CPU is a flip-chip package with a metallic lid, which can be directly removed by acids from the front side, as shown in Fig. 2.

Testing was conducted at nominal voltage and ambient room temperature using different data patterns. The SEU char-

Table 1. List of device under test.

Device	Function	Vendor	Process	Substrate thickness (μm)
HM628512A	512k \times 8 SRAM	Hitachi	0.5 μm	230
IDT71V416S	256k \times 16 SRAM	IDT	0.13 μm	250
MPC8548	32 bits CPU	Freescale	90 nm SOI	720

* Project supported by the Industrial Technology Development Program of China (No. A1320110028) and the National Natural Science Foundation of China (No. Y0503GA160).

[†] Corresponding author. Email: gqfeng@cssar.ac.cn

Received 5 July 2011, revised manuscript received 19 August 2011

© 2012 Chinese Institute of Electronics

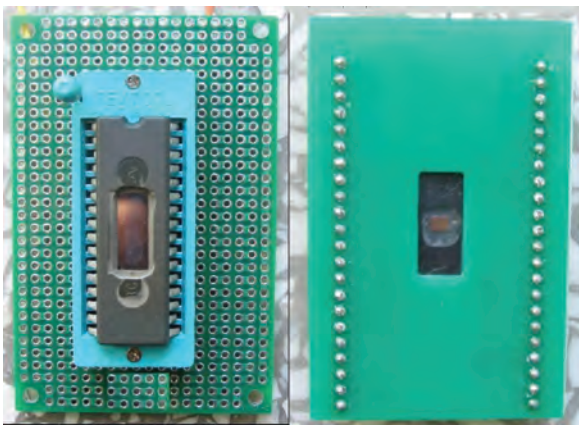


Fig. 1. Picture of samples #1 and #2 with packages opened.



Fig. 2. Picture of sample #3 with package opened.

acteristics are measured by a customized memory SEU test system. The device under test (DUT) power is supplied by using a custom designed instrument called a single event latch-up detector, which controls DUT power current and switches the power off whenever the current drawn on its power line exceeds a preset limit. The SEL current curve was measured by using a digital phosphor oscilloscope, DPO4054, equipped with a current probe.

The single event effect simulation facility utilized in this experiment is based on a pico-second pulsed laser, its main properties include wavelength of 1064 nm, pulse duration of 25 ps, spot size of 2 μm , frequency range of 1–10 kHz and maximum laser energy of 500 μJ . This tool is capable of delivering ten thousand pulses per second across a DUT over its entire surface in a fully automatic manner. The X – Y – Z motorized mechanical alignment stage with 1 μm close-loop accuracy could realize the high precision sensitivity mapping of DUT to SEE.

For the qualitative evaluation of the device under test response to SEE, a key point in SEE simulation experiment is to calculate the equivalent LET for laser pulse. If one laser pulse is equivalent to an ion of LET, the amount of charge generated

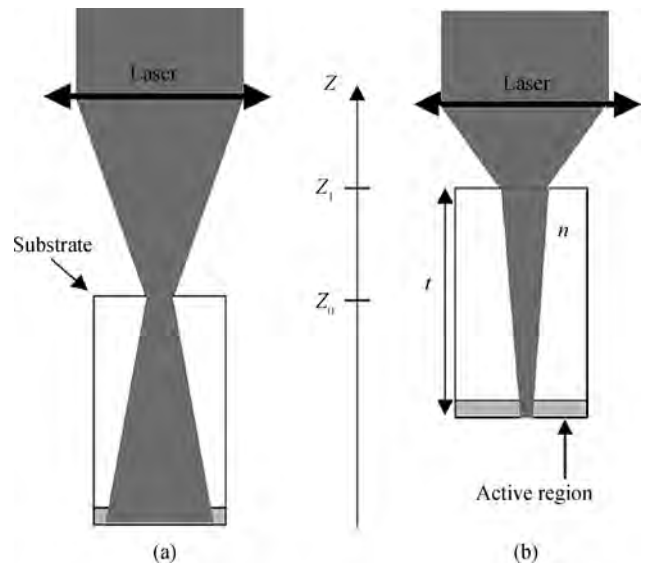


Fig. 3. Spot focused on the front side through substrate.

by an ion per unit length in the semiconductor is equivalent to that by single laser pulse. If linear absorption in semiconductor is considered alone, we get the equivalent LET equation for the laser pulse:

$$\text{LET}(x) = 10^{-20} \times \frac{\alpha \lambda E_{\text{ion}}}{\rho h c} E_{\Lambda} \exp(-\alpha x), \quad (1)$$

where α [cm^{-1}] is the absorption coefficient in the semiconductor, λ [cm] is the pulsed laser wavelength, E_{ion} [eV] is the energy required for an ion to activate a pair of electron–hole, ρ [mg/cm^3] is the density of the semiconductor, h is the Planck constant, c is velocity of light and E_{Λ} [pJ] is the energy of laser pulse.

Previous theoretical work has been performed defining an equivalent laser LET^[2, 19], which had been used to quantitatively estimate the SEE threshold LETs of some devices^[21, 22]. However, as the feature sizes scale down, the testing error between a calculated equivalent laser LET and heavy ion LET is larger. Therefore, in this work we explore an empirical relationship between laser energy threshold and heavy ion LET based on the above theory. In Section 3 this method is described in detail.

Backside studies require a spot focused on the front side sensitive volumes through silicon substrate, as shown in Fig. 3. If the laser beam is focused on the surface of the device substrate, it will naturally diverge along its optical path in the silicon, as shown in Fig. 3(a). Therefore, a shift of the focused laser from backside surface is necessary, and is dependent on the thickness of substrate (t) and the refractive index of the semiconductor (n), given by t/n according to theory about converging beam propagation in silicon shown in Fig. 3(b). For the HM628512A device, according to Eqs. (2) and (3), the shift value is near 66 μm , corresponding to a measured thickness of about 230 μm and the semiconductor refractive index of 3.5, implemented by moving the Z axis of the motorized stage.

$$Z_1 = Z_0 + \frac{t}{n}, \quad (2)$$

$$\Delta Z = Z_1 - Z_0 = \frac{t}{n}. \quad (3)$$

The experiments consist of automatically running the DUT following one laser pulse strike at an area of $2 \times 2 \mu\text{m}^2$ with known energy. Laser pulses are emitted in single shot each time while the motorized stage manually reaches a position of the pulse strike. The number and addresses of upset errors are immediately recorded including an MBU. As the supply currents exceed the threshold, the SEL detector counter is incremented and the power supply is reset within $100 \mu\text{s}$. The DUT detection and protection is achieved by the SEL detector, which compares the power currents with previously set threshold values (about five times the typical operating currents of DUT). Then, this testing process is repeated with several laser energies until SEU and SEL thresholds can be acquired.

3. Results and discussion

3.1. SEU of SRAMs

Two SRAMs are conducted in a dynamic test mode with three different data patterns—‘00H’, ‘FFH’ and ‘55H’. Firstly, test data is written in the SRAMs, and then read-rewrite operations are continuously performed during laser automatic scanning. The speed of motorized stage is set to 2 mm/s, corresponding to a laser frequency of 1 kHz, in order to have laser beam focused on complete DUT surface.

The incident energy of DUT backside surface can be directly measured with a laser energy meter. However, the efficient energy contributing to the SEE is defined as the energy available in the device sensitive region. The first effect considered is the reflection occurring on the backside of DUT. Theoretically, the coefficient of reflection for the air:silicon interface characterized by parameter R is about 36% for a 1064 nm laser. Then, the attenuation of the incident laser energy by the optical transmission of hundreds of micrometers of silicon substrate obeys Beer’s Law, $E = E_0[\exp(-\alpha t)](1 - R)(1 + T)$, where E_0 is the incident energy, t is the thickness of substrate, T is a parameter corresponding to reflection by the metal layers when arriving at the front side and E is the energy available in the device sensitive region. For commercial CMOS technology, its doping level is usually low (about 10^{17} cm^{-3}). For a wavelength of 1064 nm near silicon band gap, based on an empirical model for determining the absorption coefficient in doped silicon^[23], its absorption coefficient is about 20 cm^{-1} . In other work^[12], the factor of T has been determined to be approximately 0.45. Based on the $E = E_0[\exp(-\alpha t)](1 - R)(1 + T)$, α , t , R and T parameters, we obtain the E of threshold energy activating SEU. The deduced results are listed in Fig. 4.

From the results, we can see that different data patterns do not influence on SEU threshold and cross-section. However, there is a lower laser energy threshold and more upset errors for smaller feature size SRAM #2, as shown in Fig. 3. According to Eq. (1), the equivalent laser LET threshold of SRAM #2 is about 3 MeV·cm²/mg, which is six times larger than the heavy ion results (0.5 MeV·cm²/mg)^[12]. The problem is that the differences existing between the laser test and the heavy ion test is that the laser charge tracks are larger than the heavy-

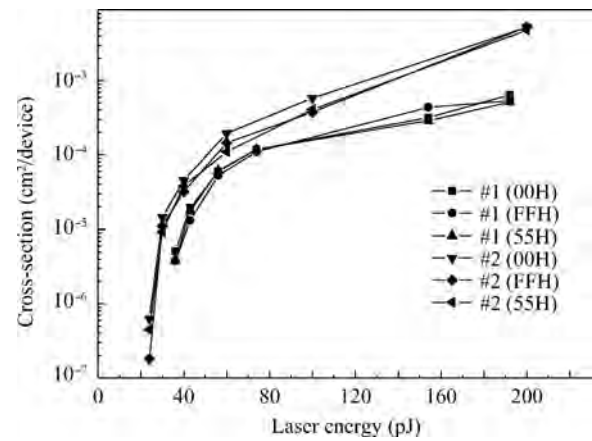


Fig. 4. Laser cross-section curves for SRAMs #1 and #2.

Table 2. List of DUT test results.

Sample	E_0 (pJ)	E (pJ)	LET _{laser} (MeV·cm ² /mg)	ΔZ (μm)
#1	3152	1636	34	66
#2	2937	1586	33	71

ion’s. Indeed, for the 1064 nm laser, it is impossible to have a laser-spot diameter smaller than $1 \mu\text{m}$ due to the diffraction limitation. A laser spot could cover more than one memory cell inducing more MBUs with high laser energy, which would not occur during particle accelerator tests. Therefore, it is necessary to choose a low energy activating cross-section as a reference point to correct the laser testing results in order to avoid any overestimation MBUs at high laser energies.

In Ref. [12], the cross-section of SRAM #1 is $7 \times 10^{-4} \text{ cm}^2/\text{device}$ in heavy ion LET of 4 MeV·cm²/mg. In our work, the cross-section $6.39 \times 10^{-4} \text{ cm}^2/\text{device}$ is corresponding to 192 pJ laser energy. Our hypothesis is that the same cross-section should have the same LET, so we can get:

$$\text{LET}_{\text{laser}} = \frac{1}{48} \times E(\text{Laser Energy}). \quad (4)$$

According to Eq. (4), we can get the equivalent laser LET threshold of #1 is 0.75 MeV·cm²/mg. The relative test error is 50% compared to the heavy ion result. The equivalent laser LET threshold of #2 is calculated to be 0.5 MeV·cm²/mg and the heavy ion experiment is planned based on that value.

3.2. SEL of SRAMs

The SEL threshold and supply current characterization of SRAM #1 and #2 are investigated with the same test procedure as the 3.1 SEU of SRAMs. The main testing results about E_0 , E , LET_{laser} and ΔZ are shown in Table 2. The equivalent laser LET threshold of #1 SRAM is calculated to be 34 MeV·cm²/mg. There is about 39% error compared to heavy ion 55.9 MeV·cm²/mg for #1 SRAM.

Of the SRAMs tested, only SRAM #1 experienced destructive SEL, resulting in burnout during non-current-limited conditions at nominal voltage. However, for the SRAM #2 with deep sub-micron feature size, a non-destructive micro SEL phenomenon is observed. The micro SEL is described as an

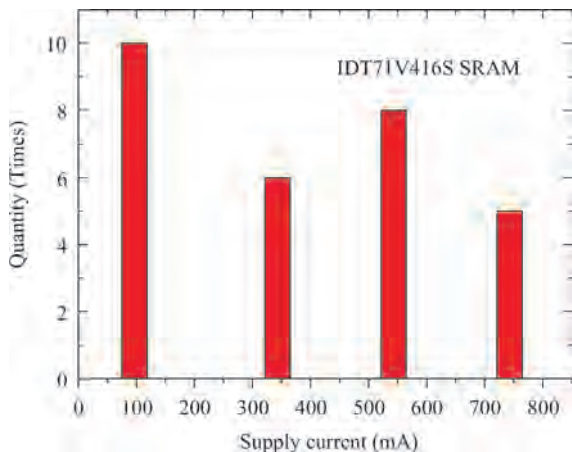


Fig. 5. Micro SEL current histogram for SRAM #2.

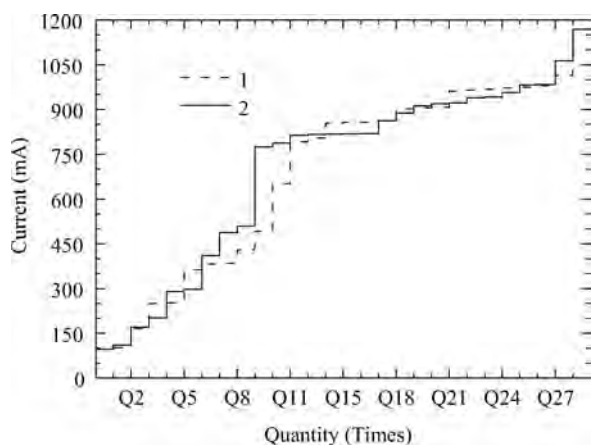


Fig. 6. Supply current with different test sequences.

SEL phenomenon locally isolated in a limited part of device chip. The remaining areas of the chip are still functional during the local SEL, because a sufficient bias voltage is supplied for those areas. Furthermore, one interesting consequence is that there are four kinds of different latch-up currents, 97, 334, 543 and 743 mA. Through the entire device scanning, there are 29 micro SEL sensitive areas, 10 for 97 mA, 6 for 334 mA, 8 for 543 mA and 5 for 743 mA shown in Fig. 5.

Moreover, test results have indicated that micro SEL has a step-by-step increase of supply current phenomena. In particular, it is found that once a micro SEL is initiated at a given location, successive laser pulses at that location lead to no further increase in the current. Charge injection at a different location leads to micro SEL effects. Figure 6 illustrates the multistep micro SEL current variation curves with two different test sequences on 29 sensitive areas. After one micro SEL occurs, the value of next micro SEL current is related to its struck location among the 29 areas. The difference is shown with line1 and line 2 in Fig. 6. After either the test sequence, the final supply current value is stable at 1175 mA after 29 areas being tested. That is because the current is limited by the device’s internal circuitry.

Since the micro SEL current is limited and not destructive, the effect on device function can be significant. In particular, for the satellite designer it is the critical nature of choosing the

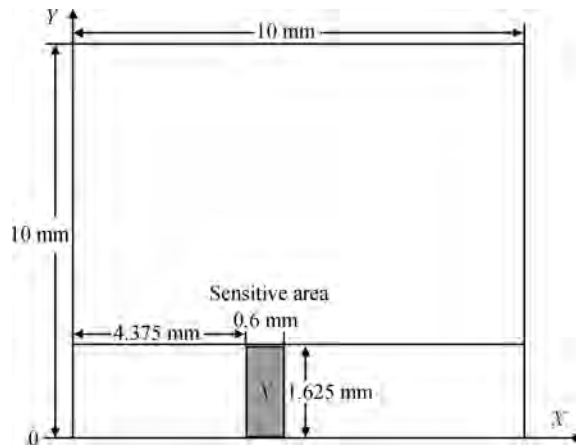


Fig. 7. SEU sensitive mapping of register for CPU #3.

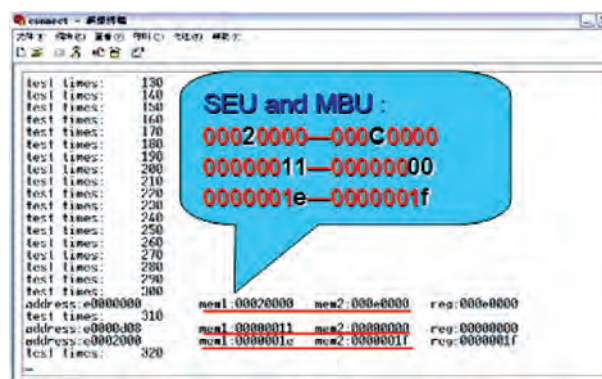


Fig. 8. SEU detecting results of register for CPU #3.

proper set point for current limitation. Otherwise a micro SEL renders the device inoperable. If the current limitation is set too high, such an event can bring about significant dead time for the electronic system. This result may be unacceptable for the mission. The pulsed laser can be an effective tool to investigate this effect in the device before the mission is launched.

3.3. SEU of CPU

The MPC8548 evaluation board is used to run the SEU detecting software. In this work, the register SEU characteristics of power PC CPU have been performed. Through the entire device scanning, the SEU sensitive mapping of the register is acquired as shown in Fig. 7, area is $0.6 \times 1.625 \text{ mm}^2$, about 0.975% of the total device area.

According to Eqs. (1) and (2), we can obtain the equivalent laser LET threshold of #3 is $2.16 \text{ MeV}\cdot\text{cm}^2/\text{mg}$. Taking into account the 90 nm feature size, the heavy ion LET threshold should be lower than the laser’s.

Although the laser spot size is larger than deep sub-micron storage cell, single event upset and multiple bit upsets (two bits) have been examined in 90 nm CPU register, as shown in Fig. 8. It is demonstrated that the pulsed laser technique can be utilized reasonably to evaluate small feature size devices.

4. Conclusion

This paper has demonstrated that the test data pattern does not influence SEU threshold and cross-section. The supply current state of micro latch-up for deep sub-micron SRAM is related to the location of device. An empirical relationship between laser energy threshold and heavy ion LET is determined based on the same cross-section. According to this empirical relationship, the estimated equivalent laser LET error for SRAM is 50% maximum. The laser energy thresholds for small feature sizes were correlated to equivalent laser LET thresholds. The relative errors will be investigated for the deep sub-micron device in a future work.

References

- [1] Johnston A H. Charge generation and collection in p-n junctions excited with pulsed infrared lasers. *IEEE Trans Nucl Sci*, 1993, 40(6): 1694
- [2] Melinger J S, Buchner S, McMorow D, et al. Critical evaluation of the pulsed laser method for single event effects testing and fundamental studies. *IEEE Trans Nucl Sci*, 1994, 41(6): 2574
- [3] Jones R, Chugg A M, Jones C M S, et al. Comparison between SRAM SEE cross-sections from ion beam testing with those obtained using a new picosecond pulsed laser facility. *IEEE Trans Nucl Sci*, 2000, 47(6): 539
- [4] Pouget V, Fouillat P, Lewis D, et al. Laser cross section measurement for the evaluation of single-event effects in integrated circuits. *Proceedings of 11th European Symposium for Reliability of Electronic Devices, Failure Physics and Analysis, Dresden, Germany, 2000: 1371*
- [5] Alpat B, Battiston R, Bizzarri M, et al. A pulsed nanosecond IR LASER diode system to automatically test the single event effects in the laboratory. *Nuclear Instruments and Methods in Physics Research A*, 2002, 485:183
- [6] Richter A K, Arimura I. Simulation of heavy charged particle tracks using focused laser beams. *IEEE Trans Nucl Sci*, 1987, 34(6): 1234
- [7] Mclean F B, Oldham T R. Charge funneling in n- and p-type Si substrates. *IEEE Trans Nucl Sci*, 1982, 29(6): 2017
- [8] Buchner S, Knudson A, Kang K, et al. Charge collection from focused picosecond laser pulses. *IEEE Trans Nucl Sci*, 1988, 35(6): 1517
- [9] Gossett C A, Hughlock W B, Hohnston A H. Laser simulation of single-particle effects. *IEEE Trans Nucl Sci*, 1992, 39(6): 1647
- [10] Technology Modeling Associates PISCES version 9033, Palo Alto, CA: Technology Modeling Associates, 1991
- [11] Lewis D, Pouget V, Beaudoin F, et al. Backside laser testing of ICs for SET sensitivity evaluation. *IEEE Trans Nucl Sci*, 2001, 48(6): 2193
- [12] Darracq F, Lapuyade H, Buard N, et al. Backside SEU laser testing for commercial off-the-shelf SRAMs. *IEEE Trans Nucl Sci*, 2002, 49(6): 2977
- [13] Amusan O A, Witulski A F, Massenqill L W, et al. Charge collection and charge sharing in a 130 nm CMOS technology. *IEEE Trans Nucl Sci*, 2006, 53(6): 3253
- [14] Musseau O, Gardic F, Roche P, et al. Analysis of multiple bit upsets (MBU) in CMOS SRAM. *IEEE Trans Nucl Sci*, 1996, 43(6): 2879
- [15] Black J D, Sternberg A L, Alles M L, et al. Multiple-bit upset in 130 nm CMOS technology. *IEEE Trans Nucl Sci*, 2005, 52(6): 2536
- [16] Page T E Jr, Benedetto J M. Extreme latchup susceptibility in modern commercial-off-the-shelf (COTS) monolithic 1M and 4M CMOS static random-access memory (SRAM) devices. *IEEE Radiation Effects Data Workshop, 2005: 1*
- [17] Shindou H, Kuboyama S, Hirao T, et al. Local and pseudo SELs observed in digital LSIs and their implication to SEL test method. *IEEE Trans Nucl Sci*, 2005, 52(6): 2638
- [18] Poivey C, Kim H, Berg M D, et al. Radiation characteristics of a 0.11 μm modified commercial CMOS process. *IEEE Radiation Effects Data Workshop, 2006: 150*
- [19] Pouget V, Lapuyade H, Fouillat P, et al. Theoretical investigation of an equivalent laser LET. *Microelectron Reliab*, 2001, 41: 1513
- [20] Huang Jianguo, Han Jianwei. The mechanism for SEU simulation by pulsed laser. *Science in China, Series G*, 2004, 47(5): 540
- [21] Moss S C, LaLumondiere S D, Scarpulla J R, et al. Correlation of picosecond laser-induced latchup and energetic particle-induced latchup in CMOS test structures. *IEEE Trans Nucl Sci*, 1995, 42(6): 1948
- [22] McMorow D, Melinger J S, Buchner S, et al. Application of a pulsed laser for evaluation and optimization. *IEEE Trans Nucl Sci*, 2000, 40(6): 559
- [23] Falk R A. Near IR absorption in heavily-doped silicon: an empirical approach. *Proceedings of the 26th International Symposium for Testing and Failure Analysis, 2000: 121*